Molecular Microbiology (2006) **61**(4), 1069–1080 doi:10.1111/j.1365-2958.2006.05295.x
First published online 21 July 2006

The biosynthetic pathway for aurofusarin in *Fusarium graminearum* reveals a close link between the naphthoquinones and naphthopyrones

Rasmus J. N. Frandsen,[1*] Nikoline J. Nielsen,[2] Nicolai Maolanon,[2] Jens C. Sørensen,[2] Stefan Olsson,[1] John Nielsen[2] and Henriette Giese[1]
Departments of [1]Ecology and [2]Natural Sciences, The Royal Veterinary and Agricultural, University, DK-1871 Frederiksberg C, Copenhagen, Denmark.

Summary

Fungal polyketide biosynthesis typically involves multiple enzymatic steps and the encoding genes are often found in gene clusters. A gene cluster containing *PKS12*, the polyketide synthase gene responsible for the synthesis of the pigment aurofusarin, was analysed by gene replacement using *Agrobacterium tumefaciens*-mediated transformation to determine the biosynthesis pathway of aurofusarin. Replacement of *aurR1* with *hygB* shows that it encodes a positively acting transcription factor that is required for the full expression of *PKS12*, *aurJ*, *aurF*, *gip1* and FG02329.1, which belong to the gene cluster. *AurR1* and *PKS12* deletion mutants are unable to produce aurofusarin and rubrofusarin. Bio- and Chemoinformatics combined with chemical analysis of replacement mutants (Δ*aurJ*, Δ*aurF*, Δ*gip1*, Δ*aurO* and Δ*PKS12*) indicate a five-step enzyme catalysed pathway for the biosynthesis of aurofusarin, with rubrofusarin as an intermediate. This links the biosynthesis of naphthopyrones and naphthoquinones together. Replacement of the putative transcription factor *aurR2* results in an increased level of rubrofusarin relative to aurofusarin. Gip1, a putative laccase, is proposed to be responsible for the dimerization of two oxidized rubrofusarin molecules resulting in the formation of aurofusarin.

Introduction

The plant pathogenic filamentous fungi *Fusarium acuminatum*, *F. avenaceum*, *F. crookwellens*, *F. culmorum*, *F. graminearum*, *F. poae*, *F. pseudograminearum*, *F. sambucinum*, *F. Sporotrichioides* and *F. tricinctum* all produce the red pigment aurofusarin, a secondary metabolite belonging to the naphthoquinone group of polyketides (Medentsev and Akimenko, 1998; Samson *et al*., 2000). Aurofusarin was first isolated from *F. culmorum* and its structure was characterized by Ashley *et al*. (1937). This pigment has antibiotic properties against both mycelial fungi and yeasts (Medentsev *et al*., 1993). In addition, Dvorska *et al*. (2001) showed that it alters the A and E-vitamin and fatty acid composition in egg yolks of Japanese quails. The function of the compound in the fungus is unresolved as white mutants have a higher growth rate than the wild type and are as pathogenic on wheat and barley (Malz *et al*., 2005).

The aurofusarin synthesis is dependent on PKS12 (Gaffoor *et al*., 2005; Kim *et al*., 2005; Malz *et al*., 2005). Fungal PKS genes are generally found to reside within clusters of tightly linked genes that encode transcription factors, transporters and enzymes required for the modification of the primary PKS product as exemplified by the aflatoxin gene cluster (Bhatnagar *et al*., 2003 and references therein). The genes are often under the regulation of a common transcription factor (Chang *et al*., 1995), and this is also the case for aurofusarin. Malz *et al*. (2005) analysed *F. pseudograminearum* mutants affected in aurofusarin production, obtained by random *Agrobacterium tumefaciens*-mediated transformation mutagenesis, and found that 10 genes surrounding *PKS12* were downregulated in mutants where T-DNA integration had occurred in the bidirectional promoter region of FG02320.1 (*aurR1*) and FG02321.1 (*aurO*). AurR1 has significant similarity to the aflatoxin/sterigmatocystin-specific transcription factor AflR from *Aspergillus* sp., and AurR1 was predicted to function as a positive acting pathway-specific transcription factor for the aurofusarin gene cluster (Fig. 1 and Table 1). According to Malz *et al*. (2005) the affected genes include two putative transcription factors (*aurR2* and *aurJ*), one pump (*aurT*), five catalytic enzymes (*PKS12*, *aurO*, *aurF*, *gip1* and *aurL2*) and two open reading frames (ORFs) that show no similarity to any characterized proteins.

Kim *et al*. (2005) showed that disruption of the laccase encoding gene *gip1* (FG02328.1) in the cluster led to a loss of aurofusarin production revealing an as yet uncharacterized yellow pigment, which was also present in the wild type. Deletion of *PKS12* (FG12040.1) resulted in a

Accepted 20 June, 2006. *For correspondence. E-mail raf@kvl.dk; Tel. (+45) 35282608; Fax (+45) 35282606.

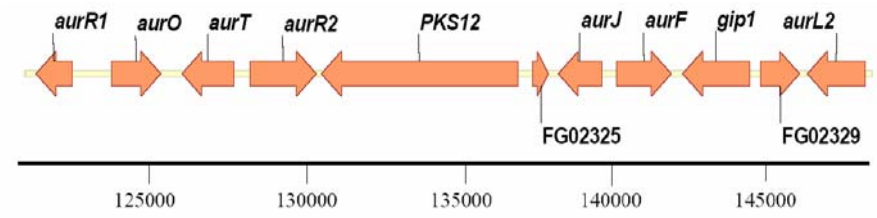

Fig. 1. The 25 kb aurofusarin gene cluster located on contig 1.116.

loss of both aurofusarin and the uncharacterized yellow pigment. Based on this, the authors conclude that PKS12 is responsible for the production of two pigments and suggest that the yellow pigment may represent an intermediate in the aurofusarin pathway.

Rubrofusarin, a second polyketide pigment isolated from *F. culmorum* and related species, also described by Ashley *et al*. (1937) and later by Tanaka and Tamura (1961), displays structural similarities to the aurofusarin monomer, and belongs to the naphthopyrone class of polyketides. Analysis of the incorporation of ^{13}C-labelled acetate in rubrofusarin by Mock and Robbers (1969) showed that rubrofusarin is formed by the condensation of seven acetate units. Leeper and Staunton (1984) determined the folding pattern of rubrofusarin (Fig. 4 folding pattern A) and noted that the relative production of aurofusarin and rubrofusarin changed under different levels of aeration. This combined with the knowledge derived from the aurofusarin gene cluster through bioinformatics, and a theoretical structural analysis of aurofusarin and rubrofusarin, led us to hypothesize that the biosyntheses of rubrofusarin and aurofusarin were interconnected.

The biosynthesis and the genetic basis for production of dimeric naphthoquinones have received little attention. Most of the chemical investigations on polyketides were carried out in the late 1970s and early 1980s and were primarily focused on the structural chemistry of polyketides. The sequencing of the *F. graminearum* genome and the development of efficient gene replacement technologies now allows genetic and biochemical studies of the rubrofusarin and aurofusarin biosynthesis in this fungus.

Our objectives in this study were to determine the function of the enzyme encoding genes found in the gene cluster, in order to propose a biosynthetic pathway for aurofusarin and the regulatory function of the putative transcription factors *aurR1*, *aurR2* and *aurJ* as suggested by Malz *et al*. (2005).

Results

Theoretical analysis of the aurofusarin biosynthesis indicates that the naphthopyrone rubrofusarin is an intermediate in the pathway

We assume that two cyclic heptaketides monomers are synthesized independently by the same molecular machinery, and then joined by an yet unidentified process to form aurofusarin. The monomer heptaketide skeleton must be synthesized by PKS12 (Gaffoor *et al*., 2005; Kim *et al*., 2005; Malz *et al*., 2005), resulting in formation of a cyclic heptaketide (nor-rubrofusarin = 5,6,8-trihydroxy-2-methyl-benzo[g]chromen-4-one) (Fig. 4). By comparing the structure of nor-rubrofusarin with the structure of the aurofusarin monomers it is apparent that it has to undergo at least four modification steps to be converted into aurofusarin: (i) methylation of the hydroxyl group found on C_8, (ii) oxidation of C_9 by introducing a hydroxyl group, (iii) further oxidation of the formed hydroxyl group on C_9 resulting in a quinone and (iv) dimerization of two monomers by oxidative coupling at C_7 atoms. PKS12 is a minimal PKS (Kroken *et al*., 2003) and tailoring enzymes are therefore required to complete the biosynthesis of aurofusarin. The four modification steps can be combined into 12 basic pathways that all equally well account for the formation of aurofusarin.

A search for metabolites that share the nor-rubrofusarin core ring structure with aurofusarin was performed at the PubChem database (http://pubchem.ncbi.nlm.nih.gov/search/). Manual inspection of the results revealed a total of 22 compounds with the desired core structure, 11 of which were monomers: kanarion, wA, rubrofusarin, quinquangulin, lambertellin, ganacin, cryptosporin, rodocladomic acid, alpha-lapachone and CID: 741831 and 11 dimeric: aurofusarin, fuscofusarin, ustilaginoidin A, aurospeone, nigerone, aurosperon D, chaetochromin, iso-chaetechromin, CID: 1598781 and CID: 1580140. Two of the identified compounds, rubrofusarin and fuscofusarin, were found to be very similar to aurofusarin. Rubrofusarin differs from nor-rubrofusarin by having a methoxy group on C_8 instead of a hydroxyl group (Fig. 4). Fuscofusarin is a heterodimeric pigment consisting of one rubrofusarin type monomer and one aurofusarin type monomer and is produced by *F. graminearum* (Takeda *et al*., 1968). The structural similarities, the co-occurrence of rubrofusarin, fuscofusarin and aurofusarin in *F. graminearum* and the shift between synthesis of aurofusarin and rubrofusarin in *F. culmorum* (Leeper and Staunton, 1984), suggest that rubrofusarin and fuscofusarin could be precursors of aurofusarin.

Table 1. The aurofusarin gene cluster in *F. graminearum*. Location of the genes on contig 1.116 and the regions replaced in this study. The predicted protein sequences were scanned for functional domains using InterPro and CDD. The predicted function is based on the bioinformatics and experimental results presented in this study. The fasciclin I family domain found in FG02329.1 does not match the domain description at InterPro, as it specifies that this domain should occur in pairs of two or four.

Locus	Name	Location	Domain(s)/motif(s)	Predicted function based on BLASTP hits and identified protein motifs	Replaced region
FG02320	*aurR1*	120517–121713	CDD14803 GAL4-like Zn2Cys6 transcription factor	Positive acting transcription factor for the aurofusarin gene cluster	120280–121626
FG02321	*aurO*	123023–124636	CDD25780 FAD binding domain CDD10151 FAD/FMN containing dehydrogenase	Oxidoreductase: catalyses the oxidation of dimeric 9-hydroxyrubrofusarin to aurofusarin	122944–124450
FG02322	*aurT*	125337–127034	CDD26721 Major facilitator (pump)	Aurofusarin/rubrofusarin pump	–
FG02323	*aurR2*[a]	127593–129769	CDD14803 GAL4-like Zn2Cys6 transcription factor CDD17436 Fungal specific TF domain	Transcription factor that possibly fine tunes the expression of the aurofusarin gene cluster	127529–129469
FG12040	*PKS12*	129934–136396	CDD27988 beta-ketoacyl synthase (KS) CDD29421 beta-Acyl carrier protein synthase (ACP) CDD25546 Acyltransferase (AT) CDD7851 Thioesterase (TE)/Claisen cyclase (Cyc)	Polyketide synthase that condensates one acetyl-CoA and six malonyl-CoA into nor-rubrofusarin, disrupted by Malz *et al*. (2005)	–
FG02325	FG02325	136921–137434	–	–	–
FG02326	*aurJ*	137754–139184	SSF46785 Winged helix DNA binding domain CDD15263 O-methyltransferase, family 2	O-methyltransferase: converts nor-rubrofusarin into rubrofusarin	137534–138773
FG02327	*aurF*	139687–141479	CDD1299 Flavin-binding monooxygenase	Monooxygenase: converts rubrofusarin into 9-hydroxyrubrofusarin	139448–141514
FG02328	*gip1*	141854–144078	CDD11840 SufI multicopper oxidase[b] CDD25500 Cu-oxidase, Multicupper oxidase	Laccase: dimerize two 9-hydroxyrubrofusarin	141985–143484
FG02329	FG02329	144432–145712	CDD24301 Four repeated domains of Fasciclin I	–	–
FG02330	*aurL2*	145967–147872	CDD11840 SufI multicopper oxidase CDD25500 Cu-oxidase, Multicupper oxidase	Laccase: not involved in aurofusarin biosynthesis	146155–148133

a. New gene structure for *aurR2* submitted under the accession number: DQ444865.
b. The identified SufI domain was not identified as a continuous motif but was interrupted by 66 aa, the same domain structure is found in the closest related protein [brown2 (gi|6090815) from *Aspergillus fumigatus*] identified by BLASTP.

The genes found in the PKS12 *gene cluster are sufficient for the complete synthesis of aurofusarin*

The genes in the cluster encode the enzymes required to catalyse the four modifications that transform nor-rubrofusarin into aurofusarin (Malz *et al*., 2005; Kim *et al*., 2006). In addition AurJ proposed to be a co-activator of the AflJ-type, also has significant similarity to OmtA (AAS90018) and to a putative O-methyltransferase from the cercosporin gene cluster (ABC79591). The search for known functional protein motifs within AurJ resulted in the identification of a 'winged-helix DNA-binding' domain and an 'O-methyltransferase family 2 (S-adenosyl-L-methionine-dependent methyltransferases)' domain (Table 1). This domain structure is shared by both OmtA and the cercosporin O-methyltransferase, but not by AflJ, suggesting that AurJ functions as an O-methyltransferase rather than as a co-activator.

In the Broad (MIT) and MIPS version of *aurR2* (FG02323.1) a binuclear zinc cluster motif is located in the first intron. The transcript was sequenced and showed that exon 1, intron 1 and exon 2 constituted a single exon of 251 bp from position 127593–127843 on contig 1.116 showing that AurR2 contains a binuclear zinc cluster (sequence deposited under accession number: DQ444865).

AurR1 is required for expression from the aurofusarin gene cluster

Agrobacterium tumefaciens-mediated transformation was used to replace *aurR1*, *aurR2* and *aurJ* with the hygromycin-resistance gene. The transformation frequencies were in the region of 200 transformants per 10^6 spores and a homologous recombination (double cross-over) frequency of 60% was estimated by counting the number of pigment mutants (*aurR1* and *aurJ* mutants). In total 46 *aurR1* replacement mutants with a white phenol-type (Fig. 3B), 111 *aurJ* mutants with a yellow/green pigmentation (Fig. 3F) and 75 *aurR2* mutants with a phenotype similar to the wild type were obtained (Fig. 3D). The homologous recombination events were confirmed by PCR with primers targeting the replaced coding sequence (type: *gene-T1/T2*) and two primer pairs located within the *hygB* gene and outside the replacement fragments (gene-T3/Hyg1 and gene-T4/Hyg2) (Fig. 2A). Southern analysis using part of the deletion vectors as probe showed that the selected replacement mutants, one of each type, only contained one copy of the hygromycin-resistance gene and that they were of the correct size (Fig. 2B). Only 5% of the examined transformants contained more than one copy of the introduced DNA.

To determine the effects on the expression of genes in the gene cluster the mutant strains were analysed by

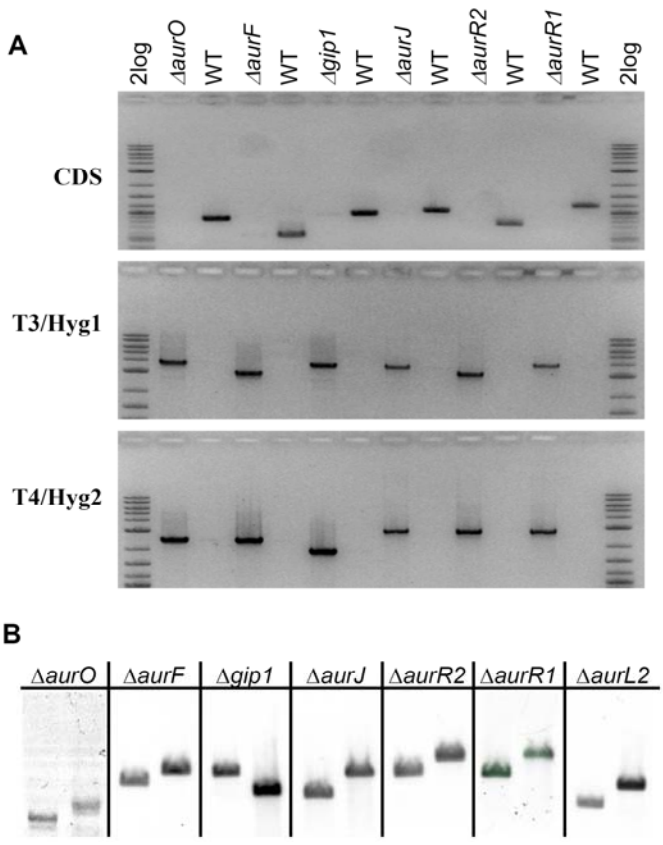

Fig. 2. A. PCR verification of targeted gene deletions. The CDS primer pairs amplify an internal fragment of the replaced sequence, which is present in the wild-type strain. The primers Hyg1 and Hyg2 anneals within the introduced *hygB* gene, while *gene*-T3 and *gene*-T4 anneals to sequences located outside the region which participates in recombination. The lack of CDS primer products in the replacement strains show that the targeted sequences have been replaced in the selected transformants. T3/Hyg1 and T4/Hyg2 primed products confirm that correct replacement has taken place. B. Southern blot analysis of the selected replacement mutants. The hybridization probes consist of the *hygB* gene and one of the two gene specific recombination flanks. The wild type is shown to the left. The observed shifts in product sizes are as expected based on the Broad genome sequence and the introduction of the *hygB* gene in the targeted loci.

RT-PCR. Replacement of *aurR1* resulted in a complete lack of transcription of the *PKS12*, *aurJ*, *aurF*, *gip1* and FG02329.1 genes (Fig. 7), confirming that AurR1 is a positive pathway-specific transcription factor. The expression of *aurT* and FG02325.1 was also affected negatively, while no significant effects were observed for *aurR2*, *aurO* or *aurL2*. Deletion of *aurJ* showed no detectable effect on gene expression in the cluster, supporting that the product of this gene acts as an O-methyltransferase rather than a co-activator. The Δ*aurR2* mutant displayed a normal expression pattern for all analysed genes, but the mycelium colour was more brown than the wild type. The co-regulation of *PKS12*, *aurJ*, *aurF* and *gip1* in the Δ*aurR1* mutant supports that these genes are involved in a common biosynthesis pathway.

aurO, aurF *and* gip1 *are required for aurofusarin production*

To test the hypothesis that the gene cluster encodes the required enzymes for the biosynthesis of aurofusarin, *aurO, aurF, gip1* and *aurL2* were replaced with *hygB*. Replacement mutants were confirmed by PCR (Fig. 2A) and Southern analysis (Fig. 2B). All selected mutants only displayed single hybridization bands showing that only one copy of the *hygB* gene had been integrated and that they were of the expected size. Gip1 has previously been deleted by Kim *et al*. (2006) resulting in a light yellow phenotype, and we found a similar phenotype (Fig. 3H). The Δ*aurF* mutant also displayed a yellow phenotype (Fig. 3G). Both mutants had a growth rate similar to the wild type. Replacement of *aurO* had no effect on the aurofusarin production when grown in DFM at 20°C (Fig. 3C) but under N-starvation, on Bell's medium, the mutant only produced rubrofusarin and its growth was inhibited. The wild-type phenotype was restored by increasing the temperature to above 25°C. No phenotypical effects were observed in the Δ*aurL2* mutant (Fig. 3I).

Nor-rubrofusarin is the primary product of PKS12

The Δ*PKS12* strain (Malz *et al*., 2005) is impaired in both aurofusarin and rubrofusarin production (Fig. 3E), as is also the case for the Δ*aurR1* mutant (Fig. 3B). However, after longer incubation periods (> 1 month) or high incubation temperatures Δ*aurR1* produced trace amounts of both compounds, probably due to a low induction-independent transcription of the required genes (data not shown). Δ*AurR2* produces relatively more rubrofusarin than aurofusarin compared with the wild type (Fig. 3D). The Δ*AurJ* strain lacks aurofusarin and rubrofusarin but produces a new yellow/green compound not present in the wild type (Fig. 3F). Characterization by UV-spectroscopy, high resolution-MS (HR-MS), 1D and 2D NMR techniques (see Figs S1 and S2 in *Supplementary material*) showed that this pigment corresponds to the unmodified cyclic heptaketide (nor-rubrofusarin) predicted to be the product of PKS12. Replacement of *aurF*, *gip1* and *aurO* resulted in mutants that produced a yellow compound, which by UV-spectroscopy, HR-MS and 1D and 2D NMR techniques was shown to be rubrofusarin (Fig. 3G and H, Figs S3 and S4 in *Supplementary material*). The HPLC analysis of the *aurL2* replacement strain did not show any significant changes compared with the wild type (Fig. 3I).

During the structural characterization of rubrofusarin, clear indications of both autooxidation and oxidative dimerization were observed. Storage of high purity rubrofusarin (exact m/z = 273.0763) in ethyl acetate at -80°C under argon atmosphere resulted in formation of trace

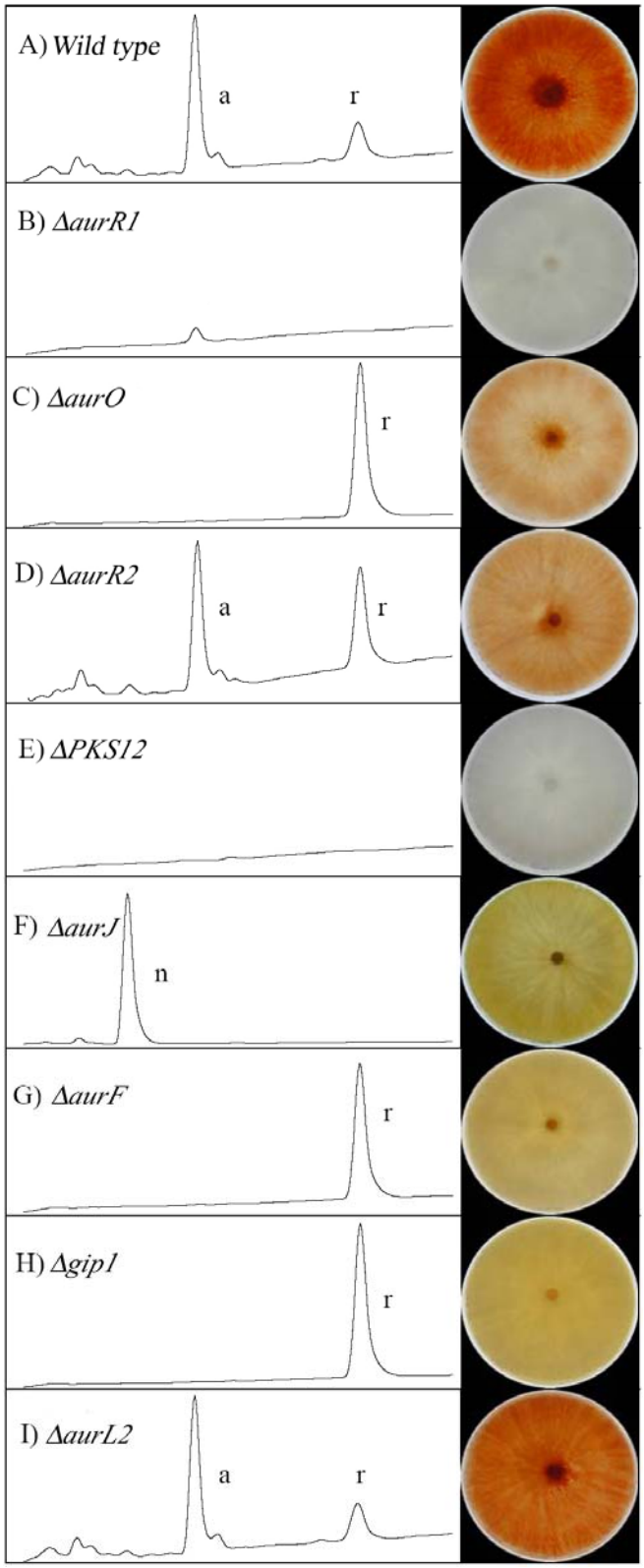

Fig. 3. Phenotype and chemotypes of the respective replacements stains. (A) wild type, (B) Δ*aurR1*, (C) Δ*aurO*, (D) Δ*aurR2*, (E) Δ*PKS12* (F) Δ*aurJ*, (G) Δ*aurF*, (H) Δ*gip1* and (I) Δ*aurL2*. The positions of aurofusarin (a), rubrofusarin (r) and nor-rubrofusarin (n) are indicated on the chromatography.

amounts of a compound with a m/z = 543, corresponding to the mass of dimerized rubrofusarin. The formation was concentration dependent. When high purity rubrofusarin was stored at 5°C in NMR-tubes with $CDCl_3$, a compound with m/z = 287.0545 was formed, corresponding to the quinone form of rubrofusarin ($C_{15}H_{10}O_6$, theoretical m/z 287.0555). The compound was not observed under similar conditions with argon atmosphere. Concentration of high purity ethyl acetate extracted rubrofusarin *in vacuo* on a rotary evaporater, resulted in trace amounts of two oxidation products ($C_{15}H_{10}O_6$, m/z = 287) and a dimeric oxidant product ($C_{30}H_{18}O_{12}$, m/z= 571). The dimeric oxidant product could be aurofusarin or another dimeric compound. Upon continuous methanol extraction from the wild type, trace amounts of a compound with a m/z of 557 was detected, this could correspond to fuscofusarin or any other $C_{30}H_{20}O_{11}$-compound ($C_{30}H_{20}O_{11}$, theoretical m/z = 556.4822).

Discussion

The aurofusarin biosynthesis pathway

PKS12 catalyses the condensation of one acetyl-CoA and six manonyl-CoA units resulting in a linear heptaketide, which is then folded into nor-rubrofusarin by the Claisen cyclase domain found in PKS12 (Fig. 3). The conversion of the ketone groups to hydroxyl groups during the cyclization is most likely the result of a non-enzymatic keto/enol tautomarization driven by the formation of the conjugated bond system within the molecule. The *aurJ* replacement mutant did not produce rubrofusarin nor aurofusarin, but instead accumulated nor-rubrofusarin, showing that AurJ catalyses the first modification of the primary PKS12 product (Fig. 4). This is in accordance with the bioinformatic analysis, which uncovered a domain structure similar to that of other O-methyltransferases involved in biosynthesis of other polyketides (Yu *et al*., 1995).

Deletion of *aurF*, *gip1* and *aurO* all resulted in the accumulation of rubrofusarin, showing that the conversion of rubrofusarin to aurofusarin requires at least three enzyme-catalysed steps. The flavin-dependent monooxygenase (AurF) must catalyse the introduction of a hydroxyl group on the C_9 of rubrofusarin resulting in formation of 9-hydroxyrubrofusarin (Fig. 4). Kim *et al*. (2005) showed that replacement of *gip1*, a putative laccase, resulted in the accumulation of a yellow compound with a higher retention time than aurofusarin. Our results show that this compound is rubrofusarin. Deletion of the second laccase in the cluster, *aurL2*, had no effects on the production of aurofusarin. Laccases have been shown to catalyse two types of relevant reactions; (i) the oxidation of hydroquinones (diphenolic compounds) similar to 9-hydroxyrubrofusarin to quinones (Marshall *et al*., 2000) and (ii) the dimerization of monomers by generation of free radicals (Claus, 2004).

The formation of carbon–carbon bonds typically requires substrate activation as seen in the reaction mechanisms of PKSs and fatty acid synthases (FAS), where the individual acetyl-CoA units are activated by carboxylation (Fujii *et al*., 2001). However, Barton and Cohen (1957) proposed that new C-C bonds can be formed by the pairing of radicals produced by one-electron oxidation of phenols, a process which can be catalysed by laccases (Nezbedová *et al*., 2001). A laccase could catalyse the removal of an electron from the deprotonated C_5-OH or C_6-OH groups of nor-rubrofusarin, rubrofusarin or 9-hydroxyrubrofusarin to activate the molecules (Fig. 5). The formed reactive radical group, initially found as O*, is then free to reallocate in the molecule due to the extensive network of conjugated bonds (Fig. 5). In the aurofusarin biosynthesis it moves to the C_7 atom and a reaction between two such activated monomers will result in the formation of a C_7-C_7 bond; covalently linking the two molecules together and cancelling out the two radicals. Based on the accumulation of rubrofusarin in the *gip1* replacement strain it is likely that this putative laccase catalyses the activation of rubrofusarin or 9-hydroxyrubrofusarin ultimately resulting in dimerization (Fig. 4).

This mechanism may also explain the formation of other dimeric polyketides. The initial structural similarity search, performed at PubChem, identified 11 dimeric compounds, which share the nor-rubrofusarin core structure with aurofusarin. The individual monomer components can be divided into three classes based on which carbon atom is involved in the dimerization bond (Fig. 6). In type A, as found in aurofusarin, the carbon atom which participates in the dimerization is C_7; in type B, as found in chaetochromin it is C_9; and in type C, as found in nigerone, it is C_{10}. All three types can be explained by the radical activation mechanism as the conjugated system found in nor-rubrofusarin, rubrofusarin and 9-hydroxyrubrofusarin, facilitate free movement of the radical by simple rearrangement of electrons (Fig. 5).

It is not likely that the activated monomers are released by the activating laccases, as they would be extremely reactive. This is supported by the three different dimerization patterns identified through the chemoinformatics, where only one of the three types has been reported for each species. Based on this the involved enzymes must be regiospecific, only allowing the activated monomers to be positioned in one conformation, resulting in one type of dimerization per dimerization enzyme. Dimeric polyketides in which two dimerization types are combined have also been reported, e.g. dianhydroaurasperone C (Ikeda *et al*., 1990), and can be explained by the interaction of two laccases with different regioselective proper-

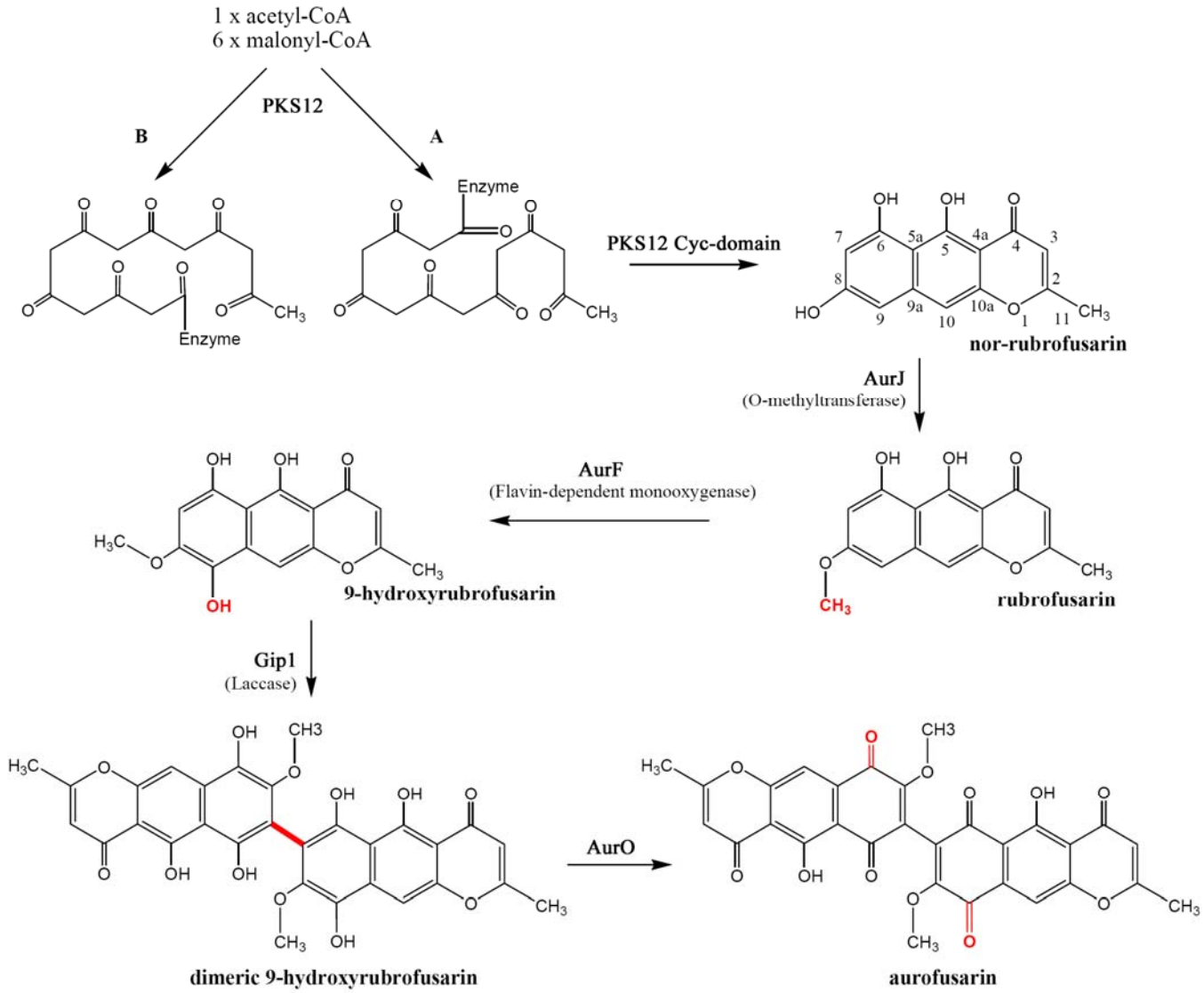

Fig. 4. The aurofusarin biosynthesis pathway and the folding pattern utilized by PKS12 to form nor-rubrofusarin. The primary product of PKS12, nor-rubrofusarin, is methylated by AurJ resulting in rubrofusarin. Rubrofusarin is then by a three-step process oxidized and subjected to dimerization catalysed by AurF, Gip1 and AurO. Only nor-rubrofusarin and rubrofusarin are stable intermediates and the order of reactions following the formation of rubrofusarin is unclear. It is possible that the last step in the reaction can occur spontaneously by UV/VIS irradiation or be driven by the formation of a conjugated bond system.

ties, resulting in an altered relative position of the two activated monomers. It is possible that the extra amino acids found in the SufI motifs of Gip1 and closely related laccases, such as Brown2 and yA, are involved in substrate positioning.

AurO contains a dehydrogenase domain and is a good candidate to catalyse the removal of hydrogen atoms from dimeric 9-hydroxyrubrofusarin resulting in the formation of aurofusarin (Fig. 4). Deletion of *aurO* resulted in the formation of rubrofusarin when the fungi were grown under nitrogen limitation and at temperatures under 25°C. The wild-type phenotype could be restored by temperatures above 25°C, possibly due to reduced substrate specificity of other oxidoreductases.

The order of reactions

The order of the two initial enzyme-catalysed steps in the biosynthesis pathway, resulting in rubrofusarin, could be determined directly, as the Δ*PKS12* and Δ*aurJ* mutants displayed unique phenotypes. This was not possible for the subsequent steps as the Δ*aurF*, Δ*gip1* and Δ*aurO* strains all accumulated rubrofusarin. The proposed order of the last three steps is based on the following biochemical and structural considerations: AurF has to act before AurO as it introduces the C_9 hydroxyl group on rubrofusarin or dimeric rubrofusarin that AurO acts on. Gip1 must function before AurO as the conjugated bond system in the quinone form of rubrofusarin is sterically locked and

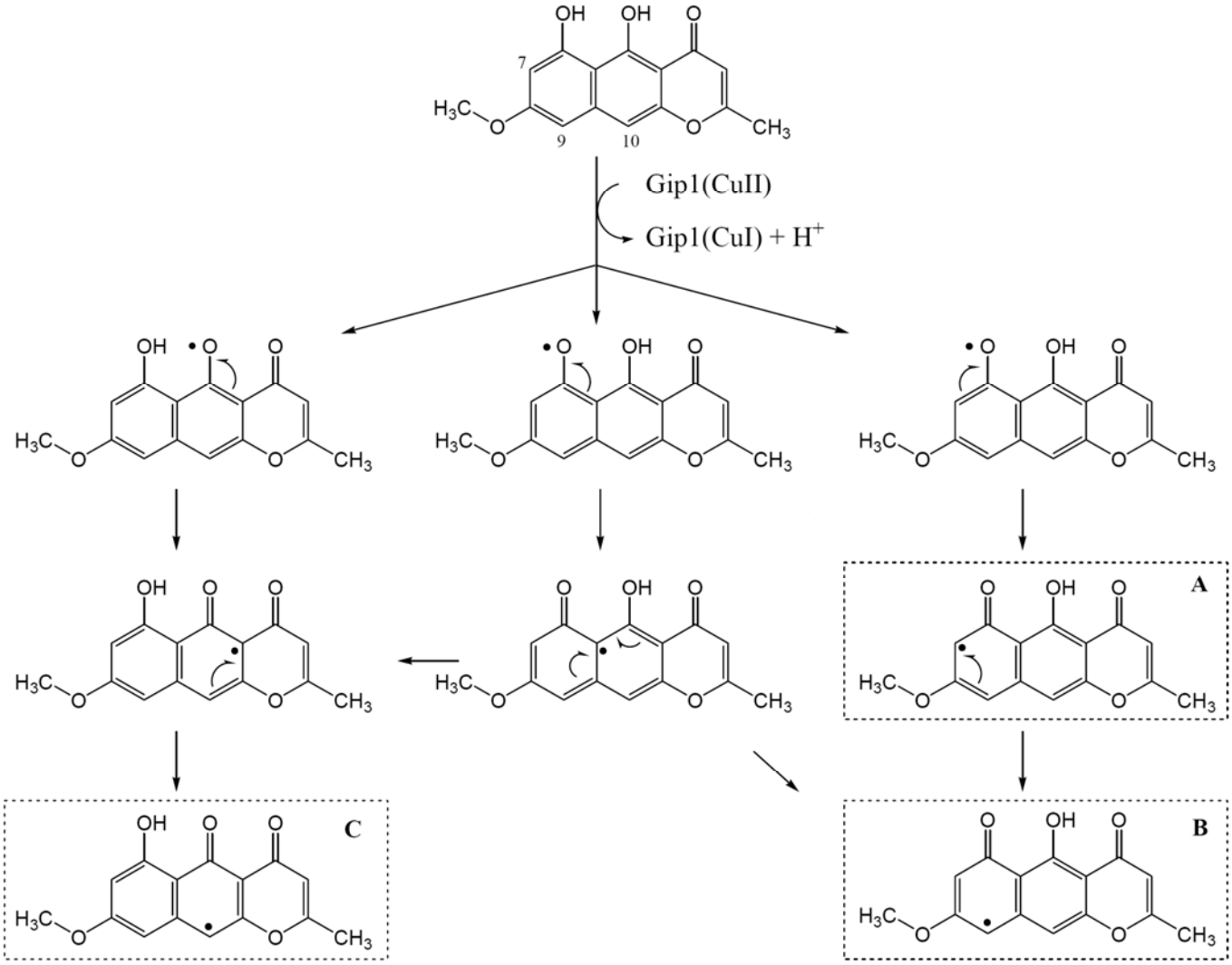

Fig. 5. Laccase-catalysed activation of monomers. An electron is removed from one of the available hydroxyl groups resulting in the formation of a bound oxygen radical. Electron rearrangement within the conjugated bond system results in activation of the C_7 position (A) in the aurofusarin biosynthesis and C_9 (B) or C_{10} (C) in other biosynthesis pathways. Reaction between two such C_7 activated monomers will result in the formation of a covalent carbon–carbon bond between the two monomers and eliminate the formed radicals. A, B and C refers to the dimerization patters shown in Fig. 6.

does not allow the free movement of electrons between the C_5 hydroxyl group and the C_7 position. If these assumptions are correct two pathways are possible: Gip1→ AurF→ AurO and AurF→ Gip1→ AurO, that from a chemical perspective are equally likely.

The heterodimeric compound fuscofusarin can be formed by the dimerization of rubrofusarin monomers with different degrees of oxidation. Either by (i) dimerization of rubrofusarin and 9-hydroxyrubrofusarin or (ii) dimerization of two rubrofusarin molecules followed by oxidation of one of the monomers by AurF and AurO. The low amounts of fuscofusarin reported by Takeda *et al*. (1968) compared with aurofusarin, suggest either that formation of fuscofusarin is an unlikely event or that it is an intermediate which is produced faster than it is converted into aurofusarin.

Rubrofusarin can undergo in vitro *chemical transformations*

During the structural determination oxygen and temperature-dependent autooxidation of rubrofusarin was observed, see Fig. S5 in *Supplementary material*. In addition dimerization of rubrofusarin and oxidized rubrofusarin to yield both homo and heterodimers were also observed, as compounds with the expected mass of dimeric rubrofusarin, aurofusarin and fuscofusarin was detected, see Fig. S6 in *Supplementary material*. The formed dimers could constitute a mixture of the following dimerization patterns: AA, AB, AC, BB, BC and CC, as the intramolecular relocation (Fig. 6) of radicals within rubrofusarin could occur under *in vitro* conditions. The low compound concentration did not allow structural determination.

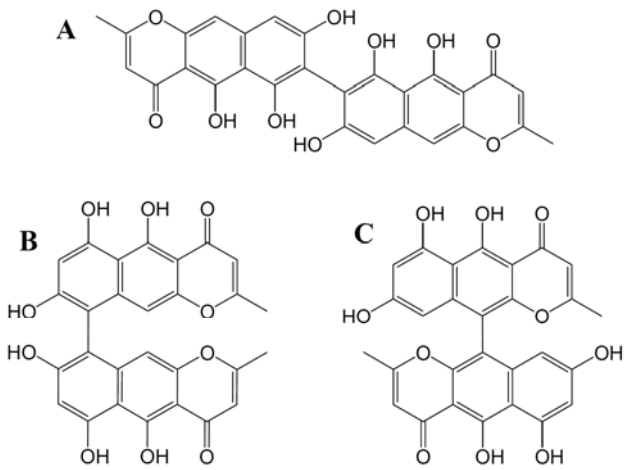

Fig. 6. The three identified dimerization patterns for heptaketides with the nor-rubrofusarin core structure can all be explained by the laccase-catalysed radical dimerization mechanism presented in Fig. 5. Type (A) found in aurofusarin, type (B) in chaetochromin and type (C) in nigerone

AurR1 and potentially AurR2 regulate expression of the aurofusarin gene cluster

Three genes were predicted by Malz *et al*. (2005) to encode transcription factors or co-regulatory factors (*aurR1*, *aurR2* and *aurJ*). This analysis showed that AurR1 and AurR2 are transcription factors of the binuclear zinc cluster class. Replacement of *aurR1* resulted in a milky white phenotype and no transcripts of the *PKS12*, *aurJ*, *aurF, gip1* and FG02329.1 genes could be detected by semiquantitative RT-PCR (Fig. 7). Kim *et al*. (2006) obtained a similar phenotype by disruption of *aurR1* (*gip2*) in a different strain of *F. graminearum*. Northern analysis did not detect any transcript from the genes located between *aurR1* and *aurL2* (Fig. 1), except for *aurO*, which was upregulated compared with the wild type. The discrepancies compared with the results in this study may be explained by differences in transcription detection limits, strains and culture conditions. Results from both experiments shows that the expression of *aurO* is not under the control of AurR1 and another regulatory system must be involved. The two novel genes, FG02325.1 and FG02329.1, are regulated by AurR1 and could potentially be involved in the biosynthesis of aurofusarin, but targeted deletions are required to determine this.

Replacement of *aurR2* resulted in a higher rubrofusarin to aurofusarin ratio compared with the wild type (Fig. 3D). Sequencing of cDNA showed that the *aurR2* transcript includes a binuclear zinc cluster and the resulting protein can probably interact directly with DNA and affect transcription. Leeper and Staunton (1984) reported that the relative amounts of rubrofusarin and aurofusarin changed with aeration of liquid cultures. Deletion of *aurR2* (this study) also resulted in a change in the ratio between aurofusarin and rubrofusarin production. It is possible that AurR2 acts as a co-regulator of AurR1 and fine tunes the biosynthesis pathway to produce rubrofusarin, aurofusarin and fuscofusarin in different levels. This would allow the producing organism to alter the proportion of the different compounds in response to changing environmental conditions such as oxygen levels and other abiotic factors. AurR2 could either function by repressing the expression of early genes in the biosynthesis pathway (*PKS12* and *aurJ*) or by increasing the expression of later genes (*aurF*, *gip1* and *aurO*) required for the conversion of rubrofusarin to aurofusarin and fuscofusarin. No effects

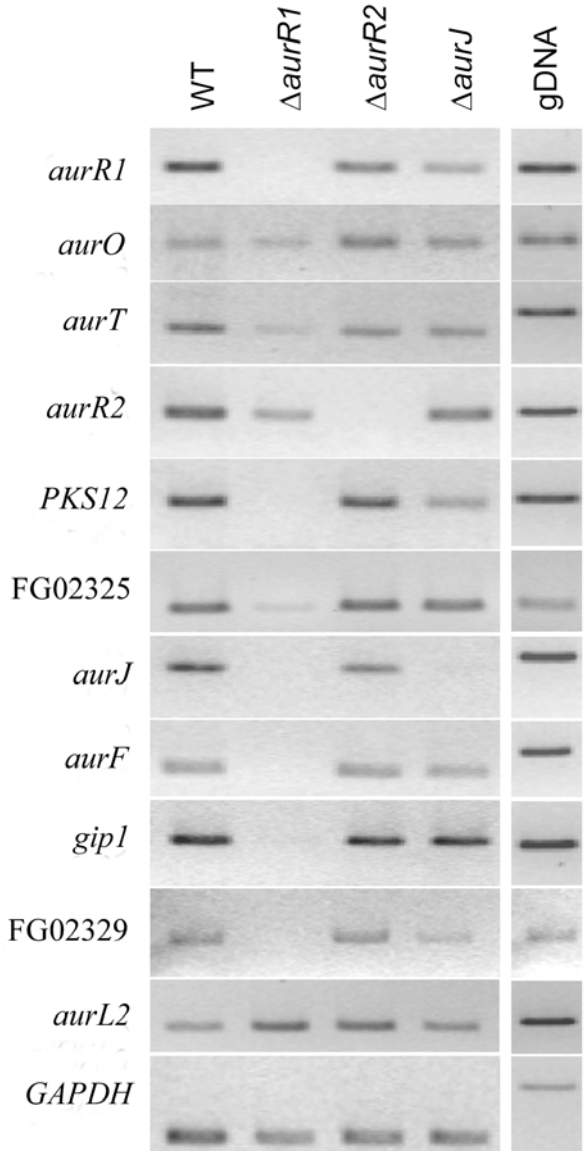

Fig. 7. RT-PCR analysis of gene expression from the aurofusarin gene cluster in the Δ*aurR1*, Δ*aurR2* and Δ*aurJ* mutant strains. The genes are displayed in the same order as in the gene cluster. No expression is observed from the *PKS12*, *aurJ*, *aurF*, *gip1* and FG02329.1 genes in the Δ*aurR1* strain, while the *aurT* and FG02325.1 is downregulated.
No effects on expression are observed in the Δ*aurR2* and Δ*aurJ* strains. The GAPDH control shows that no genomic DNA was present in the cDNA samples.

on the expression of the genes in the gene cluster were observed (Fig. 7). If AurR2 indeed functions as a co-regulator it may not be detectable by semiquantitative RT-PCR or the genes are regulated before or after the tested time point. The expression of the individual genes in the mutant should be analysed by real-time PCR to resolve this question.

Evolution of naphthopyrone and naphthoquinone PKS gene clusters

The conversion of nor-rubrofusarin into aurofusarin demonstrates for the first time a direct link between the naphthopyrone and naphthoquinone biosynthesis pathways, both with respect to the involved enzymes and genomic organization. Theoretical analysis (Medentsev and Akimenko, 1998) of the folding pattern of heptaketide naphthazarins shows that this group of naphthoquinones also must originate from naphthopyrone precursors, as no folding pattern of heptaketides will allow for a para-conformation of ketone groups. No PKSs have to our knowledge yet been linked to any of the known naphthazarins found in *F. graminearum*. This group of heptaketides has a slightly different folding pattern from that of nor-rubrofusarin and it is very likely that the PKSs involved in their biosynthesis are similar to the WA type PKSs (Bingle *et al*., 1999) and other PKSs that catalyses the condensation of a starter unit with six malonyl-CoA units, e.g. the aflatoxin and melanin PKSs in *Aspergillus* sp. (Watanabe *et al*., 1998; 2000; Tsai *et al*., 2001). Based on this the first naphthoquinone gene clusters probably have evolved from naphthopyrone gene clusters by adopting a monooxygenase and dehydrogenase to form the corresponding quinone.

Experimental procedures

Fungal strains and culture conditions

Fusarium graminearum PH-1 (NRRL 31084) was obtained from the Agriculture Research Service Culture Collection, National Center for Agricultural Utilization Research, Peoria, IL, USA. Wild-type *F. graminearum* strain 8/1 and the Δ*PKS12* of 8/1 (Malz *et al*., 2005) was obtained from W. Schaefer, University of Hamburg, Germany. The fungi were stored in 10% glycerol at -70°C and grown in the dark on minimal medium (DFM) (Malz *et al*., 2005) at 20–25°C for production of fungal material used for transformation and DNA extraction. For expression analyses fungi were cultivated on the medium described in Bell *et al*. (2003) with maltose as the C-source and urea as the N-source for 5 days at room temperature. The material was harvested and kept at -70°C until RNA extraction. For standard HPLC analyses the fungi were cultivated on Bells medium for 14 days prior to extraction as described in Malz *et al*. (2005). For the compound identification agar and mycelia were separately harvested from thirty 9-cm plates, stored at -80°C and freeze dried for 48 h or more, depending on the water content and porosity of the samples. Freeze dried agar was homogenized by blending using a model Speedy Pro from Krups. Mycelium was homogenized using mortan and pestle. All material was stored at -80°C until extraction.

Bacterial strains, vector constructions and A. tumefaciens*-mediated transformation*

The pGEM-T Easy cloning procedure (Promega) and Super chemical competent *Escherichia coli* JM109 cells were used to obtain the target *F. graminearum* sequences. *A. tumefaciens* strain LBA4404, carrying the virulence plasmid pTi4404, was used as host for the binary vector pAg1-H3 (Zhang *et al*., 2003), obtained from Dr J. S. Tkacz, Merck Research Laboratories, Rahway, USA.

Primer pairs amplifying 1.5–2 kb flanking regions of the targeted genes were designed using PrimerSelect v5.03 (DNASTAR, Madison, WI, USA) and the *F. graminearum* PH-1 genome sequence, Broad Institute (MIT) with restriction sites (Table S1) for insertion into the pAg1-H3 vector (Zhang *et al*., 2003). Primers were purchased from Invitrogen Laboratories (Portland, OR, USA) and restriction enzymes from New England Biolabs (Bererly, MA, USA). PCR reactions were performed using the following conditions; 94 °C for 5 min, 30x (94°C for 30 s, optimal annealing temperature for 30 s, 72°C for 1 min per 1 kb) and 72°C for 10 min. Flanking fragments was synthesized with the proof-reading Accuzyme DNA polymerase (BioLine, Randolph, MA, USA) mixed with 2.5 mM $MgCl_2$, 0.2 mM dNTP, 1 μl 10x PCR buffer and 20 ng gDNA in a volume of 25 μl. PCR products were purified using QIAgen PCR-purification kit (Qiagen, Chatsworth, CA, USA). 3′-A overhang was added to 2 μl purified PCR product by applying 5 units Sigma DNA polymerase, 2.5 mM $MgCl_2$, 0.2 mM dATP, 1 μl 10x PCR buffer to a final volume of 10 μl, and incubated for 40 min at 70°C. The fragments were cloned in pGEM-T Easy, positive clones were identified by colony-PCR and subsequently confirmed by sequencing, GATC Biotech Hamburg Deutschland.

pAg1-H3 and pGEM-T Easy::*gene*-A1/A2 vectors were subjected to double digestion using appropriate enzymes (Table S1), followed by TAE gel-purification using the QIAgen Gel-Extraction kit. After ligation with T4 DNA ligase for 1 h at room temperature (New England Biolabs), pAg1-H3::*gene*-A1/A2 was transformed into JM109 and plated on to LB medium with kanamycin (25 μg ml^{-1}) as selection factor. Positive transformants were identified by colony-PCR and confirmed by using restriction sites. The second flanking fragment was introduced into the pAg1-H3::*gene*-A1/A2 vector as described above to obtain pAg1-H3::*gene*-A1/A2/A3/A4.

For introduction of the *aurO*-A1/A2 fragment into the pAg1-H3::*aurO*-A3/A4 *in vivo* bacterial homologous recombination (Xi-cloning) was used, as described by Liang *et al*. (2005). The *aurO*-A1/A2 fragment was PCR-amplified using the *aurO*-A1H/A2H primers, which includes 30 bp overhangs similar to the sequences surrounding the SmaI site of pAg1-H3::*aurO*-A3/A4, allowing directional cloning. The pAg1-H3::*aurO*-A3/A4 vector was digested with SmaI to obtain blunt ends and dephosphorylated (New England Biolabs). Twenty microlitres of *E. coli* JM109 chemical competent cells

was transformed with 600 μg PCR product and 200 μg vector.

The replacement constructs were electroporated into *Agrobacterium tumefaciens* LBA4404 using a GENE PULSII from Bio-Rad (1.5 μF, 2.5 kV and 200 Ω). *A. tumefaciens*-mediated transformation was carried out as described in Malz *et al*. (2005). Hygromycin-resistant colonies and pigment mutants were recorded.

Bio- and chemoinformatics

BLASTP (release 2.2.13) searches were performed with defaulted setting at NCBI (National Center for Biotechnology Information) (Altschul *et al*., 1997). Deduced protein sequences retrieved from MIPS (http://mips.gsf.de/genre/proj/fusarium/, Mewes *et al*., 2004) were analysed with InterPro-Scan (Apweiler *et al*., 2001) and NCBI Conserved Domain Database (CDD) (Marchler-Bauer *et al*., 2005) to identify previously described functional motifs. For determiation of catalytic potential enzymes was analysed at Brenda (release 5.2) using the MIPS gene models (Schomburg *et al*., 2004). The PubChem database hosted at NCBI was used to identify compounds which display similarities to aurofusarin and rubrofusarin.

Characterization of mutants

Replacements resulting in pigment-deficient mutants were selected and confirmed using the microwave colony-PCR method (Tendulkar *et al*., 2003), with the primer pairs *gene-T1/T2*, gene-T3/HYG-1 and gene-T4/HYG-2 (see Table S1). DNA was prepared from approximately 0.9 g of fungal biomass of the wild type, PH1, and mutants, Δ*aurR1*, Δ*aurR2,* Δ*aurJ,* Δ*lacc1,* Δ*aurL2*, Δ*aurF* and Δ*aurO* according to the protocol in Malz *et al*. (2005). Southern blot analyses were performed according to the standard protocol described in Sambrook *et al*. (1989) using the following PCR fragments of the respective pAg1-H3 replacement vectors, including the *hygB* gene, as probes: *aurR1*-A4/Hyg588L (Δ*aurR1*); Hyg789U/*aurR2*-A1 (Δ*aurR2*); *aurJ*-A4/Hyg588L (Δ*aurJ*); Hyg789U/*gip1*-A4 (Δ*gip1*); *aurL2*-A1/Hyg789L (Δ*aurL2*); *aurO*-A1/Hyg588L (Δ*aurO*) and *aurF*-A1/Hyg789L (Δ*aurF*). The probes were labelled with the ECL random prime detection system, Amersham Biosciences. Genomic DNA was digested with HindIII (Δ*aurR1*), MfeI (Δ*aurR2* and Δ*aurL2*), SalI (Δ*aurJ*), StuI (Δ*gip1*), SspI (Δ*aurO*) and NruI (Δ*aurF*), that cut outside the replaced region resulting in a band shift in the mutants compared with the wild type.

RNA extraction and RT-PCR was carried out as described in Malz *et al*. (2005). The same primers for genes in the *PKS12* cluster were used with the addition of primers targeting FG02325.1, FG02329.1 and FG02330.1 (Table S1).

Chemical characterization of mutants

Chemical analyses of the wild-type 1/8 and Δ*PKS12* (Malz *et al*., 2005), and the wild type PH1 and Δ*aurR1*, Δ*aurR2*, Δ*aurJ*, Δ*aurF,* Δ*gip1* and Δ*lac1* were carried out on 14-day-old cultures according to Smedsgaard (1997) and Malz *et al*. (2005). Procedures for extraction and analysis by HPLC-UV- MS and NMR of compounds in the mutants strains are described in the *Supplementary material*.

Acknowledgements

Ulla Rasmussen and Kirsten Henriksen are gratefully acknowledged for excellent technical assistance. Peter Stougaard is acknowledged for technical advice and critical review of the manuscript. The Danish Research Foundation, Centre for Plant–Microbe Interactions and the Danish Ministery of Food Science supported this work. Merck Research Laboratories are acknowledged for the pAg1-H3 vector.

References

Altschul, S.F., Madden, T.L., Schaffer, A.A., Zhang, J., Zhang, Z., Miller, W., and Lipman, D.J. (1997) Gapped BLAST and PSI-BLAST: a new generation of protein database search programs. *Nucleic Acids Res* **25:** 3389–3402.

Apweiler, R., Attwood, T.K., Bairoch, A., Bateman, A., Birneym, E., Biswas, M., *et al.* (2001) The InterPro database, an integrated documentation resource for protein families, domains and functional sites. *Nucleic Acids Res* **29:** 37–40.

Ashley, J.N., Hobbs, B.C., and Raistrick, H. (1937) Studies in the biochemistry of micro-organisms. LIII. The crystalline coloring matters of *Fusarium culmorum* (W. G. Smith) Sacc. and related forms. *Biochem J* **31:** 385–397.

Barton, D.H.R., and Cohen, T. (1957) *Festschrift Professor Dr. Arthur Stoll*. Basel: Birkhäuser, pp. 117–144.

Bell, A.A., Wheeler, M.H., Liu, J.G., and Stipanovic, R.D. (2003) United States Department of Agriculture – Agricultural Research Service studies on polyketide toxins of *Fusarium oxysporum* f sp vasinfectum: potential targets for disease control. *Pest Manag Sci* **59:** 736–747.

Bhatnagar, D., Ehrlich, K.C., and Cleveland, T.E. (2003) Molecular genetic analysis and regulation of aflatoxin biosynthesis. *Appl Microbiol Biotechnol* **61:** 83–93.

Bingle, L.E.H., Simpson, T.J., and Lazarus, C.M. (1999) Ketosynthase domain probes identify two subclasses of fungal polyketide synthase genes. *Fungal Genet Biol* **26:** 209–223.

Chang, P.K., and Ehrlich, K.C., Yu, J., Bhatnagar, D., and Cleveland, T.E. (1995) Increased expression of *Aspergillus parasiticus aflR*, encoding a sequence-specific DNA-binding protein, relieves nitrate inhibition of aflatoxin biosynthesis. *Appl Microbiol Biotechnol* **61:** 2372–2377.

Claus, H. (2004) Laccases: structure, reactions, distribution. *Micron* **35:** 93–96.

Dvorska, J.E., Surai, P.F., Speake, B.K., and Sparks, N.H. (2001) Effect of the mycotoxin aurofusarin on the antioxidant composition and fatty acid profile of quail eggs. *Br Poult Sci* **42:** 643–649.

Fujii, I., Watanabe, A., Sankawa, U., and Ebizuka, Y. (2001) dentification of Claisen cyclase domain in fungal polyketide synthase WA, a naphthopyrone synthase of *Aspergillus nidulans*. *Chem Biol* **8:** 189–197.

Gaffoor, I., Brown, D.W., Plattner, R., Proctor, R.H., Qi, W., and Trail, F. (2005) Functional analysis of the polyketide synthase genes in the filamentous fungus *Gibberella zeae*

(anamorph *Fusarium graminearum*). *Eukaryot Cell* **4:** 1926–1933.

Ikeda, S., Sugita, M., Yoshimura, A., Sumizawa, T., Douzono, H., Nagata, Y., and Akiyama, S. (1990) *Aspergillus* species strain M39 produces two naphtho-gamma-pyrones that reverse drug resistance in human KB cells. *Int J Cancer* **45:** 508–513.

Kim, J.-E., Han, K.-H., Jin, J., Kim, H., Kim, J.-C., Yun, S.-H., and Lee, Y.-W. (2005) Putative polyketide synthase and laccase genes for biosynthesis of aurofusarin in *Gibberella zeae*. *Appl Environ Microbiol* **71:** 1701–1708.

Kim, J.E., Jin, J., Kim, H., Kim, J.C., Yun, S.H., and Lee, Y.W. (2006) GIP2, a putative transcription factor that regulates the aurofusarin biosynthetic gene cluster in *Gibberella zeae*. *Appl Environ Microbiol* **72:** 1645–1652.

Kroken, S., Glass, N.L., Taylor, J.W., Yoder, O.C., and Turgeon, B.G. (2003) Phylogenomic analysis of type I polyketide synthase genes in pathogenic and saprobic ascomycetes. *Proc Natl Acad Sci USA* **100:** 15670–15675.

Leeper, F.J., and Staunton, J. (1984) The biosynthesis of rubrofusarin, a polyketide naphthopyrone from *Fusarium culmorum*: 13C N.M.R. assignments and incorporation of 13C- and 2H-labelled acetates. *J Chem Soc Perkin Trans* **I12:** 2919–2925.

Liang, X., Teng, A., Chen, S., Xia, D., and Felgner, P.L. (2005) Rapid and enzymeless cloning of nucleic acid fragments. United States Patent no. 6,936,470. B2.

Malz, S., Grell, M.N., Thrane, C., Maier, F.J., Rosager, P., Felk, A., *et al.* (2005) Identification of a gene cluster responsible for the biosynthesis of aurofusarin in the *Fusarium graminearum* species complex. *Fungal Genet Biol* **5:** 420–433.

Marchler-Bauer, A., Anderson, J.B., Cherukuri, P.F., DeWeese-Scott, C., Geer, L.Y., Gwadz, M., *et al.* (2005) CDD: a conserved domain database for protein classification. *Nucleic Acids Res* **33:** D192–D196 (Database Issue).

Marshall, M.R., Kim, J., and Wei, C.-I. (2000) Enzymatic browning in fruits, vegetables and seafoods. FAO rapport. Medentsev, A.G., and Akimenko, V.K. (1998) Naphthoquinone metabolites of the fungi. *Phytochemistry* **47:** 935–959.

Medentsev, A.G., Kotik, A.N., Trufanova, V.A., and Akimenko, V.K. (1993) Identification of aurofusarin in *Fusarium graminearum* isolates, causing a syndrome of worsening of egg quality in chickens. *Prikl Biokhim Mikrobiol* **29:** 542–546.

Mewes, H.W., Amid, C., Arnold, R., Frishman, D., Guldener, U., Mannhaupt, G., *et al.* (2004) MIPS: analysis and annotation of proteins from whole genomes. *Nucleic Acids Res* **32:** D41–D44.

Mock, B.H., and Robbers, J.E. (1969) Biosynthesis of rubrofusarin by *Fusarium graminearum*. *J Pharm Sci* **58:** 1560–1562,.

Nezbedová, L., Hesse, M., Drandarov, K., Bigler, L., and Werner, C. (2001) Phenol oxidative coupling in the biogenesis of macrocyclic spermine alkaloids aphelandrine and orantine in *Aphelandara* sp. *Planta* **213:** 411–417.

Sambrook, J., Fritsch, E.F., and Maniatis, T. (1989) *Molecular Cloning: A Laboratory Manual*, 2nd edn. Cold Spring Harbor, NY: Cold Spring Harbor Laboratory Press.

Samson, R.A., Frisvad, J.C., and Hoekstra, E.S. (2000) *Introduction to Food- and Airborn Fungi*, 6th edn. Utrecht, NL: Centraalbureau voor schimmelcultures.

Schomburg, I., Chang, A., Ebeling, C., Gremse, M., Heldt, C., Huhn, G., and Schomburg, D. (2004) BRENDA, the enzyme database: updates and major new developments. *Nucleic Acids Res* **32:** D431–D433 (Database Issue).

Smedsgaard, J. (1997) Micro-scale extraction procedure for standardized screening of fungal metabolite production in cultures. *J Chromatogr A* **760:** 264–270.

Takeda, T., Morishita, E., and Shibata, S. (1968) Metabolic products of fungi. XXX. The structure of fuscofusarin. *Chem Pharm Bull* **16:** 2213–2215.

Tanaka, H., and Tamura, T. (1961) The chemical constitution of rubrofusarin. *Tetrahedron Lett* **4:** 151–155.

Tendulkar, S.R., Gupta, A., and Chattoom, B.B. (2003) A simple protocol for isolation of fungal DNA. *Biotechnol Lett* **25:** 1941–1944.

Tsai, H.F., Fujii, I., Watanabe, A., Wheeler, M.H., Chang, Y.C., Yasuokam, Y., *et al.* (2001) Pentaketide melanin biosynthesis in *Aspergillus fumigatus* requires chain-length shortening of a heptaketide precursor. *J Biol Chem* **276:** 29292–29298.

Watanabe, A., Ono, Y., Fujii, I., Sankawa, U., Mayorga, M.E., Timberlake, W.E., and Ebizuka, Y. (1998) Product identification of polyketide synthase coded by *Aspergillus nidulans* wA gene. *Tetrahedron Lett* **39:** 7733–7736.

Watanabe, A., Fujii, I., Tsai, H., Chang, Y.C., Kwon-Chung, K.J., and Ebizuka, Y. (2000) *Aspergillus fumigatus* alb1 encodes naphthopyrone synthase when expressed in *Aspergillus oryzae*. *FEMS Microbiol Lett* **192:** 39–44.

Yu, J., Chang, P.K., Payne, G.A., Cary, J.W., Bhatnagar, D., and Cleveland, T.E. (1995) Comparison of the omtA genes encoding O-methyltransferases involved in aflatoxin biosynthesis from *Aspergillus parasiticus* and *A. flavus*. *Gene* **163:** 121–125.

Zhang, A., Lu, P., Dahl-Roshak, A.M., Paress, P.S., Kennedy, S., Tkacz, J.S., and An, Z. (2003) Efficient disruption of a polyketide synthase gene (pks1) required for melanin synthesis through *Agrobacterium*-mediated transformation of *Glarea lozoyensis*. *Mol Genet Genomics* **268:** 645–655.

Supplementary material

The following supplementary material is available for this article online:

Fig. S1. Structure of nor-rubrofusarin.

Fig. S2. UV-spectrum of nor-rubrofusarin.

Fig. S3. Structure of rubrofusarin.

Fig. S4. UV-spectrum of rubrofusarin.

Fig. S5. *In vitro* radical initiated oxidation of rubrofusarin resulting in formation of hydroquinone and quinone forms of rubrofusarin.

Fig. S6. Possible reaction mechanism for dimerization of quinones under *in vitro* conditions.

Table S1. Primers for targeted gene replacement and verification of replacement events.

This material is available as part of the online article from http://www.blackwell-synergy.com

